Spring 2016

Tracking silver, gold, and titanium dioxide nanoparticles through drinking water systems by single particle - inductively coupled plasma - mass spectrometry

Ariel Renee Donovan

Department:

TRACKING SILVER, GOLD, AND TITANIUM DIOXIDE NANOPARTICLES THROUGH DRINKING WATER SYSTEMS BY SINGLE PARTICLE - INDUCTIVELY COUPLED PLASMA - MASS SPECTROMETRY

by

ARIEL RENEE DONOVAN

A THESIS

Presented to the Faculty of the Graduate School of the

MISSOURI UNIVERSITY OF SCIENCE AND TECHNOLOGY

In Partial Fulfillment of the Requirements for the Degree

MASTER OF SCIENCE

in

CHEMISTRY

2016

Approved by

Honglan Shi, Advisor
Yinfa Ma
Xinhua Liang

PUBLICATION THESIS OPTION

This thesis contains one paper from pages 4-30 that has been prepared in the style utilized by a publication in *Chemosphere*, V144, (2016), pages 148-153.

ABSTRACT

Single particle (SP)-ICP-MS methods were developed to characterize and quantify Ti-containing, titanium dioxide, silver, and gold NP concentration, size, size distribution and dissolved metal element concentration in surface water and treated drinking water. The effectiveness of conventional drinking water treatments (including lime softening, alum coagulation, filtration, and disinfection) to remove NPs from surface water was evaluated using six-gang stirrer jar test simulations. Six-gang stirrers were used to simulate drinking water treatments including lime softening, alum coagulation, powdered activated carbon sorption, filtration, and disinfection by free chlorine. Lime softening effectively removed most nanoparticles added. Source and drinking waters from three large drinking water treatment facilities were collected and analyzed by the SP-ICP-MS methods. Ti-containing particles and dissolved Ti were present in the river water samples, but Ag and Au were not present. The facilities were able to effectively remove most of the Ti-containing particles found in the source water.

ACKNOWLEDGMENTS

This thesis could not have been accomplished without the support of the Chemistry Department staff and faculty, Dr. Honglan Shi and her research team at Missouri S&T, and my personal support system including close family and friends.

To my family, thank you for your enduring support and love as I continue my education.

I would like to thank Dr. Honglan Shi for her educational and financial support through my undergraduate and graduate career. Without her assistance, this work would not have been possible.

This research work was supported under a cooperative agreement with PerkinElmer, Inc. (Massachusetts, USA) by providing a model NexION 300D/350 ICP-MS, and was supported by Missouri Department of Natural Resources and the Center for Single Nanoparticle, Single Cell, and Single Molecule Monitoring (CS^3M) at Missouri University of Science and Technology.

TABLE OF CONTENTS

SECTION

LIST OF ILLUSTRATIONS

Page

LIST OF TABLES

Page

1. INTRODUCTION

1.1. ENVIRONMENTAL AND HEALTH CONCERNS OF NANOPARTICLES

Nanoparticles are produced and used in increasing numbers of industrial applications each year [1]. Some of the most widely produced nanoparticles include titanium dioxide (TiO_2), silver (Ag), and gold (Au) [2]. As the nanoparticle industry continues to burgeon, the human health impacts of increased nanoparticle exposure are a growing concern. There are limited studies regarding nanoparticle toxicity to human cells. It has been shown that anatase and rutile phases of TiO_2 have different toxic effects to human dermal fibroblasts and human lung epithelial cells [3] and, in another study using human bronchial epithelial cells, the formation of reactive oxygen species (ROS) that damage the cells depends on light conditions [4]. In a comparative study between cerium dioxide (CeO_2) and Ag nanoparticles, both types of particles induced toxicity, but Ag nanoparticles resulted in more cell damage than CeO_2 nanoparticles at equivalent mass doses [5]. Ag nanoparticles have also been shown to result in cell damage, but that the extent is dose-dependent and more prominent in cancer cells [6]. There are mixed results regarding Au nanoparticle toxicity, as some research has declared them to be non-toxic while others have observed toxicity [7].

Each of the aforementioned studies evaluated nanoparticle toxicity to human cells. However, they were conducted at high nanoparticle concentrations that are outside the predicted environmental concentrations which are expected to be on the ng/L - μg/L level [8-9]. Considering the uncertainty regarding nanoparticle toxicity to human, animal, and aquatic life, it is imperative to consider the environmental occurrence of nanoparticles. It is critical to evaluate the fate of nanoparticles through anthropogenic

processes, such as waste water and drinking water treatments to fully understand their behavior, particularly when considering their inevitable environmental release [10].

1.2. NANOPARTICLE ANALYSIS BY SINGLE PARTICLE ICP-MS

Nanoparticle analysis has conventionally been done by imaging techniques such as scanning electron microscopy (SEM) or transmission electron microscopy (TEM) [11]. These techniques require extensive sample preparation for environmental samples and that the nanoparticle concentrations are high enough (mg/L levels) to observe. However, for most environmental samples nanoparticle concentrations are expected to be on the ng/L - µg/L level, orders of magnitude lower than traditional methods can evaluate [8-9]. The lack of sensitive analytical methods has hindered progression of environmental analyses of nanoparticles at environmentally relevant concentrations [12]. Single particle – inductively coupled plasma – mass spectrometry (SP-ICP-MS) is an evolving tool to detect nanoparticles at environmental concentrations directly in environmental matrices [13-19]. This technique offers the sensitivity and selectivity of traditional ICP-MS while using short dwell times to detect nanoparticle pulses. For this type of analysis samples are not acidified upon collection in order to preserve the nanoparticle. When the sample is aspirated into the plasma, nanoparticles are burst into an ion plume that then travels through the mass spectrometer and reaches the detector as a discreet packet of ions. The time it takes for the full nanoparticle pulse to reach the detector depends on the size of the nanoparticle, but will generally completely hit the detector in 0.3-0.5 ms, warranting the use of extremely short dwell times [20-22].

1.3. PROJECT OBJECTIVE

In this project three types of nanoparticles (TiO_2, Au, and Ag) were selected for monitoring through simulated drinking water treatment processes by SP-ICP-MS. Conventional drinking water treatments were simulated using six-gang stirrer apparatus to include lime softening, alum coagulation, powdered activated carbon sorption, filtration, and disinfection by free chlorine. Furthermore, samples were collected at the intake of source water and finished drinking water from three large drinking water treatment facilities in Missouri and analyzed for the selected nanoparticles by SP-ICP-MS.

PAPER

Single Particle ICP-MS Characterization of Titanium Dioxide, Silver, and Gold Nanoparticles during Drinking Water Treatment

ABSTRACT

One of the most direct means for human exposure to nanoparticles (NPs) released into the environment is drinking water. Therefore, it is critical to understand the occurrence and fate of NPs in drinking water systems. The objectives of this study were to develop rapid and reliable analytical methods and apply them to investigate the fate and transportation of NPs during drinking water treatments. Rapid single particle ICP-MS (SP-ICP-MS) methods were developed to characterize and quantify titanium-containing, titanium dioxide, silver, and gold NP concentration, size, size distribution, and dissolved metal element concentration in surface water and treated drinking water. The effectiveness of conventional drinking water treatments (including lime softening, alum coagulation, filtration, and disinfection) to remove NPs from surface water was evaluated using six-gang stirrer jar test simulations. The selected NPs were nearly completely (97 ± 3%) removed after lime softening and alum coagulation/activated carbon adsorption treatments. Additionally, source and drinking waters from three large drinking water treatment facilities utilizing similar treatments with the simulation test were collected and analyzed by the SP-ICP-MS methods. Ti-containing particles and dissolved Ti were present in the river water samples, but Ag and Au were not present. Treatments used at each drinking water treatment facility effectively removed over 93% of the Ti-containing particles and dissolved Ti from the source water.

1. Introduction

Nanoparticles (NPs) are used in many commercial products that, during use or after disposal, can lead to their release into waste and natural waters (Benn and Westerhoff, 2008; Kaegi et al., 2008; Kaegi et al., 2010; Nowack et al., 2012; Windler et al., 2012). It is estimated that TiO_2 and Ag NP concentrations in the environment will be in the ng/L-µg/L range (Mueller and Nowack, 2008; Gottschalk et al., 2009) and are expected to increase as NP production increases. Therefore, assessing NP behavior under environmental conditions is critical as NPs in source water for drinking water may pose a direct exposure route for human ingestion of NPs. It has been reported that uncoated NPs tend to aggregate slowly with time in natural waters but remain in suspension (Keller et al., 2010; Tso et al., 2010) possibly due to the stabilizing effect of natural organic material (NOM) (Zhang et al., 2009; Thio et al., 2011).

Water treatment is the primary means to remove contaminants from drinking water, including organic compounds and suspended matter. Coagulation processes are well-known and used to remove these contaminants, but their ability to remove NPs from water has not been well established. Several studies have been conducted to determine TiO_2 and/or Ag NPs removal during alum or ferric based coagulation (Zhang et al., 2008; Chalew et al., 2013; Wang et al., 2013; Zhang, 2013). TiO_2 and Ag NP breakthrough were reported between 3-60% and 2-20%, respectively, depending on the complexity of the water (synthetic versus natural water) and treatment optimization. One study determined that microfiltration, an advanced drinking water treatment, resulted in only 0-4% and 0-2% of TiO_2 and Ag NP breakthrough, respectively (Chalew et al., 2013). However, due to the lack of analytical methods to characterize and quantify NPs at environmentally relevant concentrations, acid digestion was used during sample

preparation of analysis in each study; the state of the particles during and after treatment was unidentified. It is imperative to develop analytical methods and to conduct future studies using methodologies that can directly monitor NPs during conventional drinking water treatment processes. Single particle – inductively coupled plasma – mass spectrometry (SP-ICP-MS) is an evolving tool for NP analysis in environmental matrices. SP-ICP-MS can characterize and quantify NPs at predicted environmental concentrations directly while simultaneously measuring dissolved metal element content (Loeschner et al., 2013; Lee et al., 2014; Mitrano et al., 2014; Montano et al., 2014; Cascio et al., 2015; Dan et al., 2015b), making the rapid tracking the fate of NPs during drinking water treatment process possible. The theory behind SP-ICP-MS analysis has been described in detail elsewhere and will not be discussed here (Degueldre and Favarger, 2003; Mitrano et al., 2012; Laborda et al., 2014),

The objectives of this study were: 1) to develop rapid SP-ICP-MS methods for detecting Au-, Ag-, and Ti-containing NPs in surface and drinking water; 2) to simulate conventional drinking water treatments for tracking fate of NPs during each water treatment step; and 3) to screen the occurrence of NPs and the corresponding dissolved metal elements in source and drinking water from drinking water treatment facilities (DWTFs).

2. Materials and Methods

2.1. Materials and instrumentation

Citrate-capped Au NPs (at 50, 80, and 100 nm diameter) and Ag NPs (at 40, 70, 100 nm diameter) suspended in 2 mM sodium citrate were acquired from nanoComposix, Inc. (San Diego, CA). TiO_2 particles of 100 nm and 160 nm diameter were obtained from

US Research Nanomaterials, Inc. (Houston, TX). TiO_2, Ag, and Au NPs used in the drinking water treatment simulations were characterized by both SEM (160 nm TiO_2 particles only) and SP-ICP-MS. A representative SEM image obtained for TiO_2 particles and SP-ICP-MS measurements for each NP suspended in ultra-pure water can be found in Appendix A: Supporting material. Dissolved Ag and Ti standards (PerkinElmer, Waltham, MA) and dissolved Au standard (High-Purity Standards, Charleston, SC) were used for dissolved element calibrations. Sodium hydroxide (caustic), trace metal grade nitric acid, and aluminum sulfate ($Al_2(SO_4)_3 \cdot 14.3H_2O$) were purchased from Thermo Fisher Scientific Inc. (Pittsburgh, PA). Trace metal grade sulfuric acid and sodium hypochlorite were purchased from Sigma-Aldrich (St. Louis, MO). Hydrodarco B (HDB) powdered activated carbon (PAC) was purchased from Cabot (Marshall, TX). Ultra-pure water was generated by a Simplicity185 water purification system from Millipore. Whatman #40 filter paper was purchased from GE Healthcare Biosciences (Pittsburgh, PA). A PerkinElmer (Shelton, CT) NexION 300/350D ICP-MS with Syngistix Nano Application module was used for SP-ICP-MS analysis. Dissolved organic carbon (DOC) was monitored using a TOC-L analyzer with ASI-L liquid autosampler from Shimadzu Scientific Instruments (Columbia, MD). Turbidity was measured using a TB200 Portable Turbidimeter from Orbeco-Hellige (Sarasota, FL). UV_{254} nm absorbance was monitored using a Cary 50 Conc Scanning UV/Vis Spectrophotometer from Agilent (Santa Clara, CA). A Hitachi (Tokyo, Japan) S-4700 model field emission scanning electron microscope (FESEM) with energy-dispersive X-ray spectroscopy (EDS) capability was used to image and confirm elemental composition of NPs used during drinking water treatment simulations.

2.2. SP-ICP-MS analysis and data processing

Masses of $^{46.952}$Ti (7.3% abundance, used to avoid calcium interference at 48 amu, instrumental mass resolution of 0.7 amu), $^{106.905}$Ag, and $^{196.967}$Au were monitored by SP-ICP-MS methods developed. Previous studies have shown that a single NP results in a signal duration between 0.3-0.5 ms and that using sub ms dwell times allow for peak profiling (Laborda et al., 2011; Montaño et al., 2014). Therefore, the dwell time used was 0.1 ms with data collected over 100 s. Dissolved element calibrations were prepared for Au, Ag, and Ti in 0.45 μm nylon membrane filtered river water to match matrix. Citrate-capped Au NPs and Ag NPs were used as particle calibration standards to prevent dissolution or aggregation.

2.3. Drinking water treatment simulation by six-gang stirrer jar test

A programmable six-gang stirrer (Phipps & Bird, Richmond, VA) was used to sequentially simulate lime softening, alum coagulation with PAC sorption, and disinfection. Missouri River water was collected and refrigerated unfiltered in pre-cleaned polypropylene bottles for use in jar tests. The river water was analyzed for Au, Ag, and Ti NPs, dissolved ions, DOC, UV_{254} nm absorbance, turbidity and pH before use in jar tests and after each treatment step during the simulation. NPs (100 nm Au, 100 nm Ag, or 160 nm TiO_2) were added to 2-L of Missouri River water at 1×10^6 particles/mL and dispersed by stirring for 1 min at 100 rpm before a sample was taken. Excess lime softening was conducted with a dose of 260 mg/L as $Ca(OH)_2$ to reach pH 11. The water was mixed rapidly at 300 rpm for 30 s, mixed slowly to form floc for 10 min each at 58, 42, and 28 rpm, and allowed to settle for 180 min before another sample was taken for analysis. The water was then decanted into a new 2-L square beaker, leaving only solids behind. Alum coagulation (60 mg/L as $Al_2(SO_4)_3{\cdot}14.3H_2O$, Zone 4 coagulation at pH 7-

8) with simultaneous PAC sorption by HDB (20 mg/L) was simulated on the softened water using the same stirring parameters as softening. The pH was quickly adjusted to 8 using trace metal grade sulfuric acid during flocculation. After settling, another sample was taken for analysis and 1-L of the water was filtered by Whatman #40 filter paper (sampled after filtration) and transferred to a new 2-L square beaker for disinfection. Sodium hypochlorite solution was added to obtain a residual concentration of 2 to 4 mg/L as Cl_2, and the final sample was taken for analysis after 60 minutes of stirring at 28 rpm.

2.4. Water sample collection

Three DWTFs were selected for NP monitoring (referred to as Facilities 1, 2, and 3). Each facility used Missouri River water as source water (Facility 1 uses a blend of ground water and river water) and employed lime softening, ferric coagulation, PAC sorption and chloramine disinfection treatment techniques. Detailed information on specific treatments used at each DWTF as well as schematics for each can be found in Supplementary material. Source and drinking water samples were collected in pre-cleaned 125 mL polypropylene bottles without additives or filtration and immediately brought back to our labs for SP-ICP-MS analysis on the same day.

3. Results and Discussion

3.1. SP-ICP-MS method performance

ICP-MS instrument parameters for single particle analysis of Ti, Ag, and Au NPs are presented in Table 1. Due to the frequent and increasing use of TiO_2 NPs (Chen and Mao, 2007; Weir et al., 2012), Ti-containing particle analysis was conducted as if the Ti-NPs in water were TiO_2 NPs. Though the Ti-containing particles in water samples may not have been in the form of TiO_2 NPs, they were treated as such in this study. The NP

size detection limits (DLs) were determined to be five times the standard deviation of counts in ultra-pure water blanks analyzed against the calibration curves to ensure all false positives were removed. Minimum size DLs were 65-70 nm for TiO_2 NP, 21-23 nm for Ag NP, and 27-30 nm for Au NP. Dissolved DLs for each element were determined to be the lowest spiked concentration that maintained regression linearity ($R^2 > 0.99$) over the calibration range of 0-10 μg/L in single particle analysis mode. A blank subtraction was used in the dissolved Ti calibration to omit Ti present in the river water from the calibration intensity. Dissolved element DLs were determined to be 0.75, 0.10, and 0.10 μg/L for Ti, Ag, and Au, respectively, in river water. The dissolved DLs were higher than those obtained in traditional ICP-MS due to the short dwell time of 0.1 ms as well as matrix effects. $^{46.952}$Ti (7.3% abundance) was used to avoid $^{47.952}$Ca interference with $^{47.948}$Ti (74% abundance) (instrumental mass resolution of 0.7 amu) thus size DL was higher than that obtained by $^{47.948}$Ti used for sunscreen analysis (Dan et al., 2015a).

3.2. Nanoparticle removal during simulated drinking water treatment

Water samples used for the simulated treatment were characterized at each treatment step for DOC, pH, turbidity, and UV_{254} nm absorbance. DOC and turbidity were 2.38±0.25 mg/L and 12.53±1.58 NTU (n=6), respectively. Initial pH was 8.28±0.02 (n=6), and UV_{254} nm absorbance was 0.1636±0.0036. During the simulated water treatment, DOC, turbidity, and UV_{254} nm absorbance were reduced after softening to 16%, 97%, and 67%, respectively and were further reduced after alum coagulation to 51%, 99%, and 80%, respectively. pH increased to 11.16±0.02 (n=6) after lime softening and was reduced to pH 8.22±0.40 (n=6) after subsequent alum coagulation. Little change was observed for all parameters after filtration and disinfection.

Size distribution histograms for TiO_2 NPs during the simulated drinking water treatment are presented in Figure 1. Ti-containing particles (treated as TiO_2 NPs in this study) in the Missouri River water were evaluated to understand how the particles were affected by each treatment step. Figure 1(a) showed a wide size distribution of TiO_2 NPs in the Missouri River water. Figure 1(b) depicts the change in size distribution histogram after each treatment step when 160 nm TiO_2 NPs were added. The TiO_2 particle addition made the NP size shift to larger size range (Figure 1(b) "After Spike"), indicating that the added particles were interacting with the TiO_2 NPs present in the water and/or aggregation of the added TiO_2 particles. After lime softening, the large TiO_2 signals disappeared and a small peak near ~73 nm was observed. The nature of this peak was unknown and may have been attributed to an effect of the pH increasing to above 11 or an increase in aggregation from NPs below the DL (<64 nm) during flocculation. However, the particles present after treatment had minimal mass content compared to the original TiO_2 NPs. Dissolved Ti (which included particulate Ti below the particle size detection limit) was reduced from 7.99±0.7 µg/L (n=6) to below the DL. Alum coagulation with simultaneous PAC (HDB) sorption further reduced the particles present (Figure 1 "After Alum Coagulation + PAC"). Filtration and disinfection had no further observable effect on Ti content in the river water which was likely due to the removal of detectable particle and dissolved Ti prior to these treatments.

To evaluate the behavior of Ag and Au NPs during the simulated drinking water treatment, 100 nm Ag and 100 nm Au NPs were added to the water samples because Ag and Au NPs were not present in the Missouri River water collected for this analysis. The size distribution histograms for 100 nm Ag and 100 nm Au NPs during the simulated

drinking water treatment are presented in Figure 2. After the addition of Ag and Au NPs, the size distribution was similar to the distribution of the NPs standard in ultra-pure water (refer to Figure S5 in Appendix A: Supporting material), indicating that the particles were not aggregating or dissolving in the real water matrix. After lime softening, Ag NPs were removed (Figure 2(a)) similarly to the TiO_2 NPs with the appearance of a small peak at size ~34 nm. The source of this peak was unclear, but it was possible that some of the added particles stayed in suspension and were partially dissolved under the softening conditions. However, further treatment by alum coagulation with simultaneous PAC sorption (HDB) removed the remaining small Ag NPs. No further effects were observed on Ag NPs during the following filtration and disinfection, which, as with the TiO_2 NPs, was most likely due to NP removal during the previous treatment steps. Added 100 nm Au NPs (Figure 2 (b)) were removed during lime softening without the appearance of another small sized peak. Alum coagulation with PAC sorption removed the remaining NPs to below the DL. No further change was observed in the following filtration and disinfection, possibly for the same reason of absence of Ag NPs in the water during these treatments. Dissolved Ag and Au were also monitored during the treatments, and their concentrations remained below DLs at each step, indicating no dissolution of these NPs.

It has been shown that DOC above 4 mg/L can stabilize uncoated NPs in water matrices (Zhang et al., 2008; Zhang et al., 2009; Keller et al., 2010). Zeta-potentials have been monitored up to pH 9 for TiO_2 NPs, and indicated that as pH increased, TiO_2 NPs tended to aggregate in the presence of NOM (Thio et al., 2011). Due to DOC <4 mg/L and an increase in pH to 11.1-11.2, aggregation was expected and observed for the added TiO_2 NPs (see Figure 1(b)). Furthermore, addition of Ca^{2+} ions above 0.04 M has been

reported to induce aggregation for NPs coated in DOC (Zhang et al., 2009). In this study, after lime softening, over 89% of each type of NP was removed from the river water. Based on the $Ca(OH)_2$ added during softening (260 mg/L), the added concentration of Ca^{2+} ions (assuming dissolution) was 0.0035 M, which indicated that the removal was caused by the pH increase and floc formation and not charge stabilization induced by added Ca^{2+} ions. The results demonstrated that all of the studied NPs behaved similarly under increased pH conditions. After alum coagulation, TiO_2 NP removal was increased to over 95% and Ag and Au NPs were less than the DLs and were considered to be 100% removed. As with other monitored parameters, no significant changes occurred after filtration and disinfection because most of the NPs were removed by the softening and coagulation processes.

3.3. TiO_2, Ag, and Au nanoparticle occurrence in source water and finished drinking water of drinking water treatment facilities

To understand the fate of Ti, Ag, and Au as dissolved ions and NPs during real drinking water treatment process, each was monitored in source and drinking water from three large DWTFs in Missouri that utilize Missouri River water as source water. The results from the screening study are presented in Table 2. The quality control data (i.e., field blanks, reproducibility of duplicated samples, and sample spike recoveries) showed the good performance of the SP-ICP-MS method for both source and drinking water except TiO_2 NP spike recovery (see below). Ag and Au dissolved ions and NPs were not present in source or drinking water from any of the studied DWTFs. TiO_2 NPs were present in all source water samples. Facility 1 had the largest most frequent size of TiO_2 NPs (170 nm), while Facilities 2 and 3 had slightly smaller most frequent sizes (about 155 nm). Facility 2 and 3 had similar dissolved and Ti-containing particle concentrations

as expected due to their close location (about one mile between river intakes). Facilities 1 and 2 removed TiO_2 NPs to below DL. Facility 3 removed 93% of TiO_2 NPs, though low levels of small particles (near 76 nm) remained after the treatment; the removal differences among the three DWTFs may be explained by the differences in their treatment processes or caused by fluctuations in daily treatment. Facilities 1 and 2 both added a second dose of polymer directly before filtration, while Facility 3 added the second dose of polymer during coagulation. NPs spikes in the water samples were also evaluated. TiO_2 NPs of 100 nm size were added in the water samples. Because the standards were not surface stabilized, aggregation occurred which resulted in low particle concentration spike recoveries similar to the low recovery seen in ultra-pure water. For Facility 2, a spike was added to source water filtered by 0.45-µm nylon membrane filters to confirm the size of the added TiO_2, Ag, and Au NPs in a source water sample without high concentrations of background TiO_2 NPs or other solids. For both filtered source and drinking water, the added 100 nm TiO_2 NP size was determined to be 87 nm, or close to the 100 nm stock NP standard size, with concentration recoveries of nearly 6% that were similar to recoveries during method development, indicating that particles aggregated in the stock solution before addition to the matrix and interacted with other Ti NPs in the water (Zhang et al., 2009; Keller et al., 2010).

Ti NPs were present in the Missouri River and well water sampled during this study. Ti is one of the most abundant elements in the Earth's crust and has been observed as dissolved ions in a variety of water types (Skrabal, 1995; Skrabal, 2006). In addition to the Ti NPs that may occur naturally, the increasing use of TiO_2 and other types of NPs most likely result in environmental release. Our studies indicate that lime softening to pH

11 can remove over 89% of the Ti-containing particles and TiO_2, Ag, and Au engineered NPs. If followed by alum coagulation, Ag and Au NPs were reduced to below the DLs and over 95% of TiO_2 NPs were removed. Overall breakthrough of TiO_2 NPs was less than 5%, or less than 1 μg/L. Compared to similar studies which examined alum or ferric coagulation (Zhang et al., 2008; Chalew et al., 2013; Wang et al., 2013; Zhang, 2013), using a combination of lime softening and alum coagulation resulted in nearly total removal of NPs. When compared to microfiltration that removal NPs effectively (Chalew et al., 2013), this study indicated that conventional lime softening followed by alum coagulation resulted in similar removal efficiencies of advanced microfiltration treatments. Breakthrough concentrations into treated drinking water were below the current reported Ti values to cause cell damage in humans (Lai et al., 2008; AshaRani et al., 2009). However, as NPs are increasingly used, the environmental exposure levels are expected to increase. This study concludes that lime softening in conjunction with other typical coagulation processes will provide an efficient and available technique to remove NPs from source water of drinking water.

4. Conclusions

Here, we examined removal of Ti-containing particles found in river water and engineered TiO_2, Ag, and Au NPs during conventional drinking water treatment processes by SP-ICP-MS. Robust SP-ICP-MS methods were developed to evaluate dissolved and particulate Ti, Ag, and Au in surface and drinking water. Particle size and dissolved element detection limits were determined to be 67-70 nm (as TiO_2 NP) and 0.75 μg/L for Ti, 21-23 nm and 0.10 μg/L for Ag, and 27-30 nm and 0.10 μg/L for Au. Application of these methods allowed for direct rapid characterization of these NPs in

environmental matrices without extensive sample preparation which generated information regarding NP size, size distribution, agglomeration, and particle concentration as well as dissolved element concentrations simultaneously. Our results indicated that lime softening can effectively remove most of the NPs selected in this study, and further treatment by alum coagulation combined with PAC adsorption resulted in complete removal of Au and Ag NPs, and nearly complete removal of TiO_2 NPs. Further studies are on-going in our laboratory to elucidate removal mechanisms of NP removal and to evaluate the fate of other NPs.

Acknowledgements

We acknowledge funding received from the Missouri Department of Natural Resources for this study. The NexION 300/350D ICP-MS was provided by PerkinElmer, Inc. The authors appreciate the support from the Center for Single Nanoparticle, Single Cell, and Single Molecule Monitoring (CS^3M) at Missouri University of Science and Technology. Additionally, we would like to thank Yongbo Dan, Runmiao Xue, and Kun Liu for their support during simulated drinking water treatments and Qingbo Yang for conducting SEM imaging.

Appendix A: Supplementary Material

Drinking water treatment facility (DWTF) information

Facility 1 is located approximately 200 miles upstream from Facilities 2 and 3. Facility 2 is located just downstream of Facility 3 (the intakes of the two facilities are approximately 1 mile apart). All three facilities use Missouri River water as source water, but Facility 1 uses a blend of river and well water (more well water is used in the winter

season to increase the water temperature), as such, both river and well water were sampled at the facilities intakes to determine NPs in both types of water. Water treatment facility schematics for each facility can be seen in Figures S1, S2, and S3. Facility 1 first blends the source waters then pre-treats with a polymer (Clarifloc C-378, Polydyne) to remove most of the turbidity in primary settling basins. After pre-treatment, $KMnO_4$, ferric sulfate, lime, and monochloramine (chlorine introduction followed by ammonia, distance depends on water temperature) are added. During flocculation, PAC is added before the water reaches the secondary basins. Immediately before filtration, a second polymer dose is added as a filter-aid. Facility 2 starts treatment with lime and polymer (Robin 110, Brenntag) in a primary basin. Ferric sulfate, fluorine, and monochloramine (chlorine introduction followed by ammonia, distance depends on water temperature) are added before a second basin. Before filtration, a polyphosphate filter aid is added. Facility 3 begins river water treatment with a polymer (Clarifloc C-308P) and ferric sulfate before primary basins. Lime, additional ferric sulfate, fluoride, and monochloramine (chlorine introduction followed by ammonia, distance depends on water temperature) are added before the secondary basins and baffles. PAC is added before the water reaches a second set of baffles and, after settling, is filtered through anthracite, sand, gravel, and polymer beads.

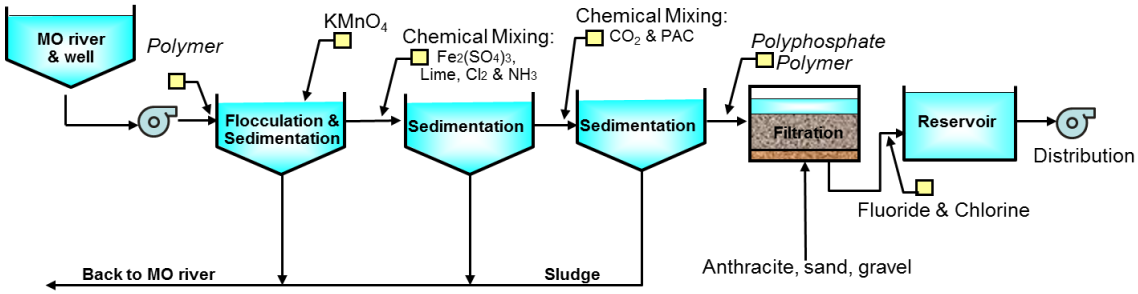

Figure S1. Full water treatment schematic of Facility 1 sampled for nanoparticle occurrence study.

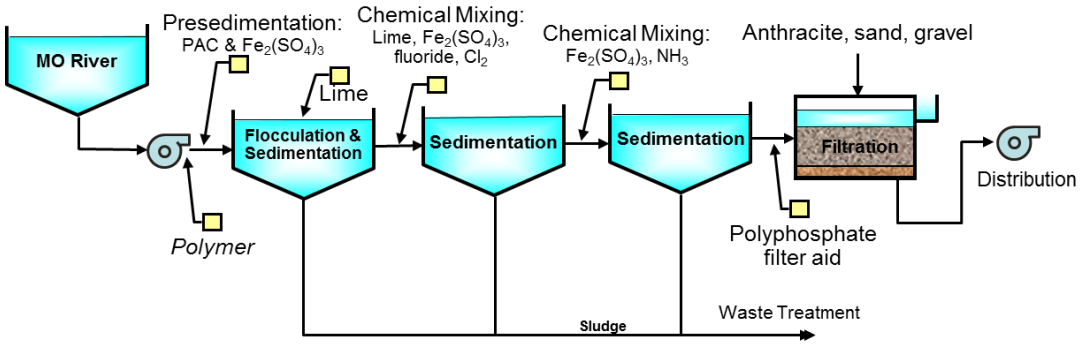

Figure S2. Full water treatment schematic of Facility 2 sampled for nanoparticle occurrence study.

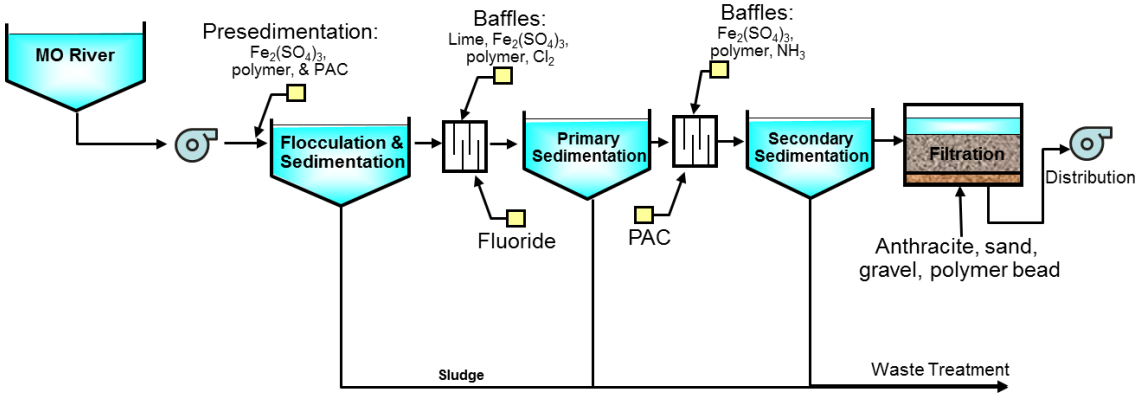

Figure S3. Full water treatment schematic of Facility 3 sampled for nanoparticle occurrence study.

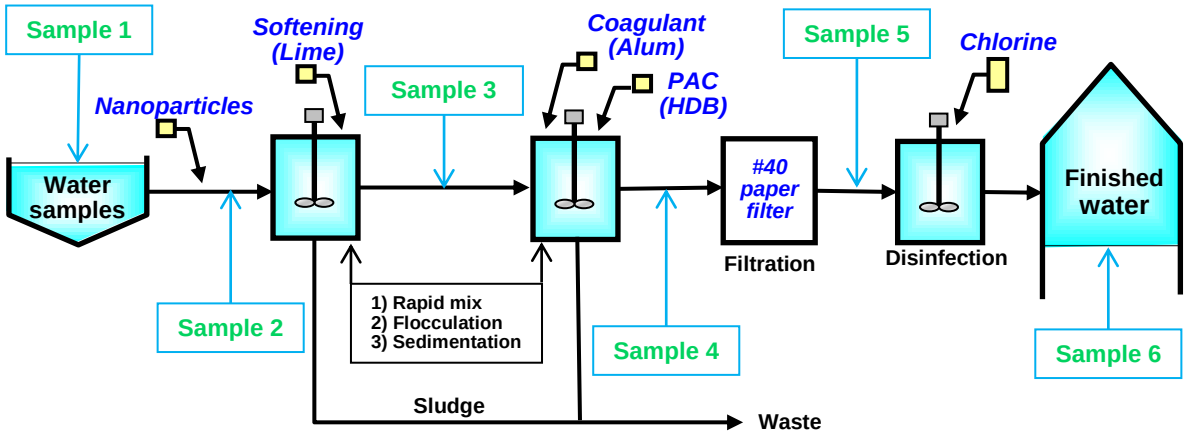

Figure S4. Schematic of simulated drinking water treatment and "sampling sites."

SEM image of 160 nm TiO_2 particles

TiO_2 SEM samples were prepared by diluting stock solutions to 10 mg/L in ultra-pure water. Each sample was ultrasonicated for 10 min to reduce aggregation before being transferred onto the SEM state (silica wafer) and the liquid was evaporated over 5 minutes. After drying, the samples were sputtered with Au/Pd and imaged under vacuum. SEM images are presented in Figure S4 for 160 nm TiO_2 particles. EDS measurements confirmed the elemental composition. TiO_2 particles exhibited aggregation after sample preparation. The particles were mostly spherical but the size distribution was not well defined and particle size varied between 100 and 250 nm.

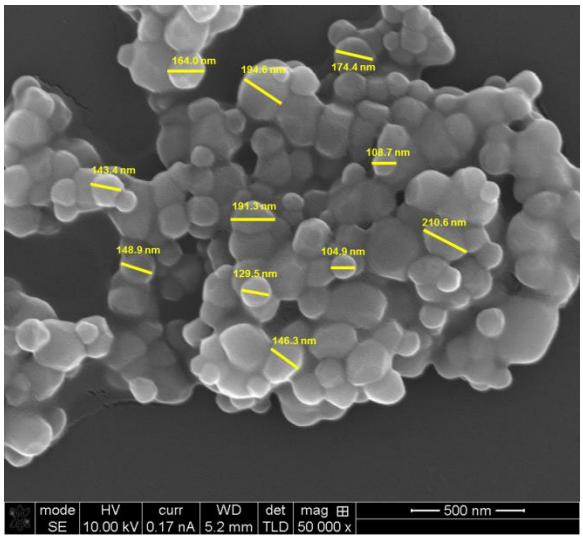

Figure S5. SEM of 160 nm TiO_2 particles.

SP-ICP-MS analysis of TiO_2, Ag, and Au NPs in ultra-pure water

NP suspensions in ultra-pure water were measured by SP-ICP-MS to determine size distributions before addition to the surface water matrix. In Fig. S5(a), the size distribution histogram of 160 nm TiO_2 indicated the particles aggregate in ultra-pure water, but the most frequent size was about 160 nm as specified. This aggregation resulted in a decrease in the particle concentration detected by the instrument, resulting in 24% particle concentration recovery. Because the particles were mostly spherical and the third power dependence on particle radius, eight particles must agglomerate in order to double the detected particle size. The variation in TiO_2 particle size coupled with the tendency to agglomerate results in the right tailing in the size distribution histogram. Both 100 nm Ag (Fig. S5(b)) and 100 nm Au (Fig. S5(c)) NPs showed well-defined size distribution histograms centered around 100 nm with good particle concentration recoveries of 98% and 91%, respectively, due to each NP being citrate-capped which prevented aggregation.

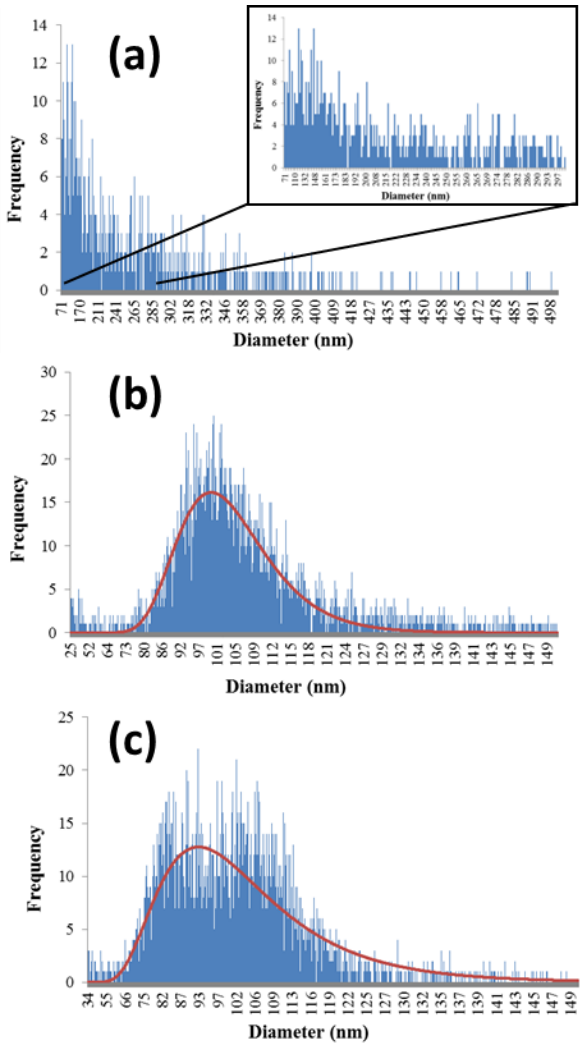

Figure S 6. Size distribution histograms of (a) 160 nm TiO_2 particles, (b) 100 nm Ag NPs, and (c) 100 nm Au NPs in ultra-pure water.

References

AshaRani, P.V., Mun, G.L.K., Hande, M.P., Valiyaveettil, S., 2009. Cytotoxicity and Genotoxicity of Silver Nanoparticles in Human Cells. ACS Nano 2, 279-290.

Benn, T.M., Westerhoff, P., 2008. Nanoparticle Silver Released into Water from Commercially Available Sock Fabrics. Environmental Science and Technology 42, 4133-4139.

Cascio, C., Geiss, O., Franchini, F., Ojea-Jimenez, I., Rossi, F., Gilliland, D., Calzolai, L., 2015. Detection, quantification and derivation of number size distribution of silver nanoparticles in antimicrobial consumer products. Journal of Analytical Atomic Spectrometry.

Chalew, T.E.A., Ajmani, G.S., Huang, H., Schwab, K.J., 2013. Evaluating Nanoparticle Breakthrough during Drinking Water Treatment. Environmental Health Perspectives 121, 1161-1166.

Chen, X., Mao, S.S., 2007. Titanium Dioxide Nanomaterials: Synthesis, Properties, Modifications, and Applications. Chemical Reviews 107, 2891-2959.

Dan, Y., Shi, H., Stephan, C., Liang, X., 2015a. Rapid analysis of titanium dioxide nanoparticles in sunscreens using single particle inductively coupled plasma–mass spectrometry. Microchemical Journal 122, 119-126.

Dan, Y., Zhang, W., Xue, R., Ma, X., Stephan, C., Shi, H., 2015b. Characterization of gold nanoparticles uptake by tomato plants using enzymatic extraction followed by single particle inductively coupled plasma-mass spectrometry. Environmental Science and Technology, DOI 10.1021/es506179e.

Degueldre, C., Favarger, P.Y., 2003. Colloid analysis by single particle inductively coupled plasma-mass spectroscopy: a feasibility study. Colloids and Surfaces A: Physicochemical and Engineering Aspects 217, 137-142.

Gottschalk, F., Sonderer, T., Scholz, R.W., Nowack, B., 2009. Modeled Environmental Concentrations of Engineered Nanomaterials (TiO2, ZnO, Ag, CNT, Fullerenes) for Different Regions. Environmental Science and Technology 43, 9216-9222.

Kaegi, R., Sinnet, B., Zuleeg, S., Hagendorfer, H., Mueller, E., Vonbank, R., Boller, M., Burkhardt, M., 2010. Release of silver nanoparticles from outdoor facades. Environmental pollution 158, 2900-2905.

Kaegi, R., Ulrich, A., Sinnet, B., Vonbank, R., Wichser, A., Zuleeg, S., Simmler, H., Brunner, S., Vonmont, H., Burkhardt, M., Boller, M., 2008. Synthetic TiO2 nanoparticle emission from exterior facades into the aquatic environment. Environmental pollution 156, 233-239.

Keller, A.A., Wang, H., Zhou, D., Lenihan, H.S., Cherr, G., Cardinale, B.J., Miller, R., Ji, Z., 2010. Stability and Aggregation of Metal Oxide Nanoparticles in Natural Aqueous Matrices. Environmental Science and Technology 44, 1962-1967.

Laborda, F., Bolea, E., Jimenez-Lamana, J., 2014. Single particle inductively coupled plasma mass spectrometry: a powerful tool for nanoanalysis. Analytical chemistry 86, 2270-2278.

Laborda, F., Jiménez-Lamana, J., Bolea, E., Castillo, J.R., 2011. Selective identification, characterization and determination of dissolved silver (I) and silver nanoparticles based on single particle detection by inductively coupled plasma mass spectrometry. Journal of Analytical Atomic Spectrometry 26, 1362-1371.

Lai, J.C.K., Lai, M.B., Jandhyam, S., Dukhande, V.V., Bhushan, A., Daniels, C.K., Leung, S.W., 2008. Exposure to titanium dioxide and other metallic oxide nanoparticles induces cytotoxicity on human neural cells and fi broblasts. International Journal of Nanomedicine 3, 533-545.

Lee, S., Bi, X., Reed, R.B., Ranville, J.F., Herckes, P., Westerhoff, P., 2014. Nanoparticle Size Detection Limits by Single Particle ICP-MS for 40 Elements. Environmental science & technology 48, 10291-10300.

Loeschner, K., Navratilova, J., Kobler, C., Molhave, K., Wagner, S., von der Kammer, F., Larsen, E.H., 2013. Detection and characterization of silver nanoparticles in chicken meat by asymmetric flow field flow fractionation with detection by conventional or single particle ICP-MS. Analytical and bioanalytical chemistry 405, 8185-8195.

Mitrano, D.M., Lesher, E.K., Bednar, A., Monserud, J., Higgins, C.P., Ranville, J.F., 2012. Detecting nanoparticulate silver using single-particle inductively coupled plasma-mass spectrometry. Environmental toxicology and chemistry / SETAC 31, 115-121.

Mitrano, D.M., Ranville, J.F., Bednar, A., Kazor, K., Hering, A.S., Higgins, C.P., 2014. Tracking dissolution of silver nanoparticles at environmentally relevant concentrations in laboratory, natural, and processed waters using single particle ICP-MS (spICP-MS). Environmental Science: Nano 1, 248-259.

Montaño, M.D., Badiei, H.R., Bazargan, S., Ranville, J.F., 2014. Improvements in the detection and characterization of engineered nanoparticles using spICP-MS with microsecond dwell times. Environmental Science: Nano 1, 338.

Montano, M.D., Lowry, G.V., von der Kammer, F., Blue, J., Ranville, J.F., 2014. Current status and future direction for examining engineered nanoparticles in natural systems. Environmental Chemistry 11, 351-366.

Mueller, N.C., Nowack, B., 2008. Exposure Modeling of Engineered Nanoparticles in the Environment. Environmental Science and Technology 42, 4447-4453.

Nowack, B., Ranville, J.F., Diamond, S., Gallego-Urrea, J.A., Metcalfe, C., Rose, J., Horne, N., Koelmans, A.A., Klaine, S.J., 2012. Potential scenarios for nanomaterial release and subsequent alteration in the environment. Environmental toxicology and chemistry / SETAC 31, 50-59.

Skrabal, S.A., 1995. Distributions of dissolved titanium in Chesapeake Bay and the Amazon River Estuary. Geochimica et Cosmochimica Acta 59, 2449-2458.

Skrabal, S.A., 2006. Dissolved titanium distributions in the Mid-Atlantic Bight. Marine Chemistry 102, 218-229.

Thio, B.J., Zhou, D., Keller, A.A., 2011. Influence of natural organic matter on the aggregation and deposition of titanium dioxide nanoparticles. Journal of hazardous materials 189, 556-563.

Tso, C.P., Zhung, C.M., Shih, Y.H., Tseng, Y.M., Wu, S.C., Doong, R.A., 2010. Stability of metal oxide nanoparticles in aqueous solutions. Water science and technology : a journal of the International Association on Water Pollution Research 61, 127-133.

Wang, H.T., Ye, Y.Y., Qi, J., Li, F.T., Tang, Y.L., 2013. Removal of titanium dioxide nanoparticles by coagulation: effects of coagulants, typical ions, alkalinity and natural organic matters. Water science and technology : a journal of the International Association on Water Pollution Research 68, 1137-1143.

Weir, A., Westerhoff, P., Fabricius, L., Hristovski, K., von Goetz, N., 2012. Titanium dioxide nanoparticles in food and personal care products. Environmental science & technology 46, 2242-2250.

Windler, L., Lorenz, C., von Goetz, N., Hungerbuhler, K., Amberg, M., Heuberger, M., Nowack, B., 2012. Release of titanium dioxide from textiles during washing. Environmental science & technology 46, 8181-8188.

Zhang, B., 2013. Removal of TiO_2 Nanoparticles by Conventional Water Treatment Processes. Environmental Engineering. Clemson University, Clemson, SC.

Zhang, Y., Chen, Y., Westerhoff, P., Crittenden, J., 2009. Impact of natural organic matter and divalent cations on the stability of aqueous nanoparticles. Water research 43, 4249-4257.

Zhang, Y., Chen, Y., Westerhoff, P., Hristovski, K., Crittenden, J.C., 2008. Stability of commercial metal oxide nanoparticles in water. Water research 42, 2204-2212.

Table 1. Instrument and method parameters for SP-ICP-MS analysis of Au, Ag, TiO_2 NPs and dissolved elements.

Instrument Parameter	**Operation Setting**		
Nebulizer	Meinhard		
Spray Chamber	Cyclonic		
Sampler Cone	Platinum		
Skimmer Cone	Platinum		
RF Power (W)	1600		
Nebulizer Gas Flow (L/min)*	1.02-1.06		
Auxiliary Gas Flow (L/min)	1.2		
Plasma Gas Flow (L/min)	18		
Sample Flow Rate (mL/min)*	0.26-0.29		
RPq	0.5		
Dwell Time (ms)	0.1		
Sample Time (s)	100		
Transport Efficiency (%)*	7.5-8.5		
Method Parameters	**Ti**	**Ag**	**Au**
Isotope (amu)	46.952	106.905	196.967
Density (g/cm^3)	4.23	10.49	19.3
Mass Fraction (%)	60	100	100
Ionization Efficiency (%)	100	100	100

*Parameter optimized daily.

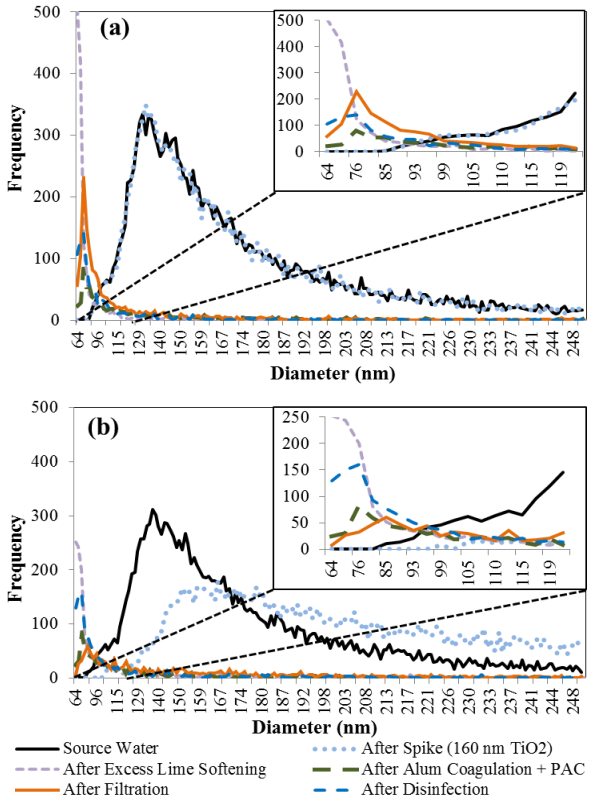

Figure 1. Combined size distribution histograms of (a) Ti-containing particles and (b) 160 nm TiO_2 particles after each step of a simulated drinking water treatment.

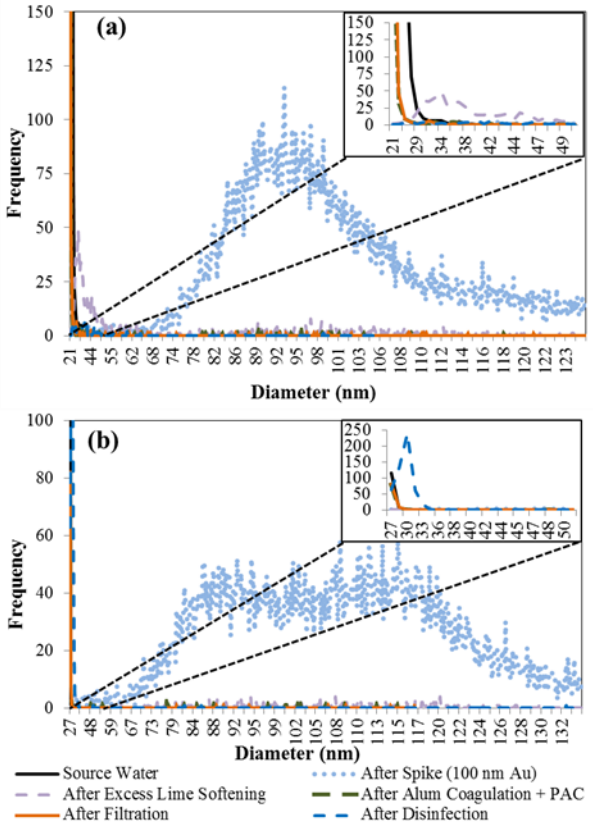

Figure 2. Combined size distribution histograms of (a) 100 nm Ag NPs and (b) 100 nm Au NPs after each step of a simulated drinking water treatment.

Table 2. Occurrence of Ti, Ag, and Au NPs and dissolved elements in source and drinking water from drinking water treatment facilities.

Sample ID	Au			Ag			Ti		
	Most Freq. Size (nm)	Part. Conc. (parts/mL)	Diss. Conc. (µg/L)	Most Freq. Size (nm)	Part. Conc. (parts/mL)	Diss. Conc. (µg/L)	Most Freq. Size (nm)	Part. Conc. (parts/mL)	Diss. Conc. (µg/L)
Facility 1*:									
Field Blank	<MDL	---	<MDL	<MDL	---	<MDL	<MDL	---	<MDL
River Water	<MDL	---	<MDL	<MDL	---	<MDL	170	431984	17.92
River Water Duplicate	<MDL	---	<MDL	<MDL	---	<MDL	168	442153	18.49
Well Water	<MDL	---	<MDL	<MDL	---	<MDL	135	14937	1.45
Well Water Spike Recovery %	98	97%	80%	98	97%	80%	102	9%	84%
Drinking Water	<MDL	---	<MDL	<MDL	---	<MDL	<MDL	<MDL	1.21
Drinking Water Duplicate	<MDL	---	<MDL	<MDL	---	<MDL	<MDL	<MDL	1.21
Facility 2:									
Field Blank	<MDL	---	<MDL	<MDL	---	<MDL	<MDL	---	<MDL
River Water	<MDL	---	<MDL	<MDL	---	<MDL	156	451473	11.68
River Water Duplicate	<MDL	---	<MDL	<MDL	---	<MDL	156	439272	10.76
River Water Spike Recovery %	97	88%	84%	97	88%	84%	87	6.1%	88%
Drinking Water	<MDL	---	<MDL	<MDL	---	<MDL	<MDL	<MDL	1.17
Drinking Water Duplicate	<MDL	---	<MDL	<MDL	---	<MDL	<MDL	<MDL	1.17
Drinking Spike Recovery %	101	94%	89%	101	94%	89%	87	5.9%	112%
Facility 3:									
Field Blank	<MDL	---	<MDL	<MDL	---	<MDL	<MDL	---	<MDL
River Water	<MDL	---	<MDL	<MDL	---	<MDL	153	424916	10.61
River Water Duplicate	<MDL	---	<MDL	<MDL	---	<MDL	159	442007	12.89
Drinking Water	<MDL	---	<MDL	<MDL	---	<MDL	76	17237	<MDL
Drinking Water Duplicate	<MDL	---	<MDL	<MDL	---	<MDL	76	15276	<MDL

*Facility 1 uses a blend of river and well water.
Spikes prepared with 2 µg/L dissolved metals and ~1×10^5 particles/mL of 100 nm Au, Ag, and TiO_2.

SECTION

2. CONCLUSION

Single particle ICP-MS methods were successfully validated in real water samples for analysis of Ti-, Au-, and Ag-containing nanoparticles. The methods were applied to the analysis of river water subjected to various drinking water treatment processes including lime softening, alum coagulation, powdered activated carbon sorption, filtration, and disinfection by free chlorine in a sequential drinking water treatment facility simulation. High nanoparticle removal was obtained after lime softening, indicating that through the increase in pH, addition of divalent cations, or the formation of other large flocs effectively removed most of the nanoparticles. Au and Ag nanoparticles were not found in the source water of the three drinking water treatment facilities collected from but Ti-containing particles were detected. For each facility, Ti-containing particles were mostly removed to below the detection limits of the SP-ICP-MS method. Through this work, single particle ICP-MS has been demonstrated to be an effective tool for monitoring nanoparticles in natural and drinking water systems.

BIBLIOGRAPHY

[1] S. Klaine, P. Alvarez, G. Batley, T. Fernandes, R. Handy, D. Lyon, S. Mahendra, M. McLaughlin, J. Lead, "Nanomaterials in the Environment: Behavior, Fate, Bioavailability, and Effects," Environmental Toxicology and Chemistry, 2008, 27, 1825-1851.

[2] R. Handy, R. Owen, E. Valsami-Jones, "The ecotoxicology of nanoparticles and nanomaterials: current status, knowledge gaps, challenges, and future needs," Ecotoxicology, 2008, 17, 315-325.

[3] C. Sayes, R. Wahi, P. Kurian, Y. Liu, J. West, K. Ausman, D. Warheit, V. Colvin, "Correlating Nanoscale Titania Structure with Toxicity: A Cytotoxicity and Inflammatory Response Study with Human Dermal Fibroblasts and Human Lung Epithelial Cells," Toxicological Sciences, 2006, 92, 174-185.

[4] J. Gurr, A. Wang, C. Chen, K. Jan, "Ultrafine titanium dioxide particles in the absence of photoactivation can induce oxidative damage to human bronchial epithelial cells," Toxicology, 2005, 213, 66-73.

[5] B. Gaiser, T. Fernandes, M. Jepson, J. Lead, C. Tyler, V. Stone, "Assessing exposure, uptake and toxicity of silver and cerium dioxide nanoparticles from contaminated environments," Environemntal Health, 2009, 8.Suppl 1, S2.

[6] P. AshaRani, G. Low Ka Mun, M. Hande, S. Valiyaveettil, "Cytotoxicity and Genotoxicity of Silver Nanoparticles in Human Cells," ACS Nano, 2009, 3, 279-290.

[7] A. Alkilany, C. Murphy, "Toxicity and cellular uptake of gold nanoparticles: what we have learned so far?," Journal of Nanoparticle Research, 2010, 12, 2313-2333.

[8] N. Mueller, B. Nowack, "Exposure Modeling of Engineered Nanoparticles in the Environment," Environmental Science and Technology, 2008, 42, 4447-4453.

[9] F. Gottschalk, T. Sonderer, R. Scholz, B. Nowack, "Modeled Environmental Concentrations of Engineered Nanomaterials (TiO2, ZnO, Ag, CNT, Fullerenes) for Different Regions," 2009, 43, 9216-9222.

[10] H. Kim, Y. Choi, K. Kim, B. Lee, J. Ranville, "Nanoparticles in the environment: stability and toxicity," Reviews on Environmental Health, 2012, 27, 175-179.

[11] M. Montaño, G. Lowry, F. Kammer, J. Blue, J. Ranville, "Current status and future direction for examining engineered nanoparticles in natural systems," Environmental Chemistry, 2014, 11, 351-366.

[12] I. Rezic, "Determination of engineered nanoparticles on textiles and in textile wastewaters," Trends in Analytical Chemistry, 2011, 30, 1159-1167.

[13] K. Loeschner, J. Navratilova, C. Kobler, K. Molhave, S. Wagner, F. Kammer, E. Larsen, "Detection and characterization of silver nanoparticles in chicken meat by asymmetric flow field flow fractionation with detection by conventional or single particle ICP-MS," Analytical and Bioanalytical Chemistry, 2013, 405, 8185-8195.

[14] S. Lee, X. Bi, R. Reed, J. Ranville, P. Herckes, P. Westerhoff, "Nanoparticle Size Detection Limits by Single Particle ICP-MS for 40 Elements," Environmental Science and Technology, 2014, 48, 10291-10300.

[15] D. Mitrano, J. Ranville, A. Bednar, K. Kazor, A. Hering, C. Higgins, "Tracking dissolution of silver nanoparticles at environmentally relevant concentrations in laboratory, natural, and processed waters using single particle ICP-MS (spICP-MS)," Environmental Science Nano, 2014, 1, 248-259.

[16] Y. Dan, H. Shi, C. Stephan, X. Liang, "Rapid analysis of titanium dioxide nanoparticles in sunscreens using single particle inductively coupled plasma-mass spectrometry," Microchemical Journal, 2015, 122, 119-126.

[17] Y. Dan, W. Zhang, R. Xue, X. Ma, C. Stephan, H. Shi, "Characterization of Gold Nanoparticle Uptake by Tomato Plants Using Enzymatic Extraction Followed by Single-Particle Inductively Coupled Plasma-Mass Spectrometry Analysis," Enviornmental Science and Technology, 2015, 49, 3007-3014.

[18] A. Donovan, C. Adams, Y. Ma, C. Stephan, T. Eichholz, H. Shi, "Single particle ICP-MS characterization of titanium dioxide, silver, and gold nanoparticles during drinking water treatment," Chemosphere, 2016, 144, 148-153.

[19] A. Donovan, C. Adams, Y. Ma, C. Stephan, T. Eichholz, H. Shi, "Detection of Zinc Oxide and Cerium Dioxide Nanoparticles during Drinking Water Treatment by Rapid Single Particle ICP-MS Methods," Analytical and Bioanalytical Chemistry, 2016, in press.

[20] C. Degueldre, P. Favarger, "Colloid analysis by single particle inductively coupled plasma-mass spectroscopy: a feasibility study," 2003, 214, 137-142.

[21] D. Mitrano, E. Lesher, A. Bednar, J. Monserud, C. Higgins, J. Ranville, "Detecting nanoparticulate silver using single-particle inductively coupled pasma-mass spectrometry," Environmental Toxicology and Chemistry, 2012, 31, 115-121.

[22] F. Laborda, E. Bolea, J. Jimenez-Lamana, "Single Particle Inductively Coupled Plasma Mass Spectrometry: A Powerful Tool for Nanoanalysis," Analytical Chemistry, 2014, 86, 2270-2278.

VITA

Ariel Donovan was born in Berlin, Germany. She completed primary and secondary school in Belton, Missouri, USA. In 2009 she was admitted to Johnson County Community College, Overland Park, Kansas, USA where she completed her associate degree in liberal arts. In 2011 she was admitted to Missouri University of Science and Technology in Rolla, Missouri, USA where she completed her bachelor degree in Chemistry in May, 2014. She continued her graduate study at Missouri University of Science and Technology in chemistry under the guidance of Dr. Honglan Shi. She received her Master of Science in Chemistry from Missouri University of Science and Technology in May, 2016.